

Imaging radar for ecosystem studies

Satellites vastly extend the surveillance of Earth's surface. Often, however, the view from space is obscured by clouds, which prevent remote sensing with optical or thermal sensors. Because of cloud cover and other inherent limitations of optical and thermal sensors, many important ecosystem properties related to structural features of the vegetation and surface moisture conditions cannot be adequately assessed. As an alternative, microwave sensors (imaging radar) have longer wavelengths (from 1 cm to 150 cm) that penetrate the densest cloud cover and are particularly sensitive to the presence of water.

To date the principal applications of imaging radar have been the mapping of geologic features and the following of seasonal changes in sea-ice. Recently a number of satellites have been launched with radar sensors, thus expanding opportunities for global assessments (Way and Smith 1991): two European Earth Remote Sensing Satellites, ERS-1 and ERS-2 (Attema 1991); a Japanese Earth Resources Satellite, JERS-1 (Nemoto et al. 1991); and, planned in late 1995, a Canadian satellite, RADARSAT (Parashar et al. 1993).

In this article we focus on the applications of imaging radar, which is a type of sensor that actively generates pulses of microwaves and, in the interval between sending pulses, records the returning signals reflected back to an antenna. The geometry of an object and its composition strongly influence the strength

Table 1. Band designations and corresponding wavelength intervals and frequency ranges for radar sensors.

Band	Wavelength range (cm)	Frequency range (GHz)
K	2.75–0.83	10.9–36.0
X	5.21–2.75	5.75–10.9
C	7.19–5.21	4.2–5.75
L	76.9–19.4	0.39–1.55
P	133.3–76.9	0.225–0.39

of the reflected microwave pulses. An important asset of radar is its ability to sense the amount of water present in or on various surfaces and whether the water is in a frozen or liquid state.

The resolution at which objects may be discerned with radar is proportional to the ratio between wavelength and antenna length. The image spatial resolution for a real aperture radar is the angular resolution multiplied by the antenna's distance from the surface. This relationship creates a problem because an instrument such as the SeaSat radar at 800-kilometers altitude and 24-centimeters wavelength would provide a resolution of 20 km with its 10-meter antenna (Curlander and McDonough 1991). To improve resolution, a synthetic aperture radar (SAR) technique is used in which the phase and magnitude of the returned echo is recorded for the entire time a feature on the earth's surface is in view of the radar. A high-resolution image is then produced in the image processing by synthesizing an extremely long antenna.

The spatial resolution of images produced by airborne SAR systems is typically in the 1–10-meter range, compared with 10–30 m for satellite SARs. The imagery is acquired at various angles and fields of view, offering a trade-off between spatial resolution and area coverage (Figure 1). The smaller the SAR viewing angle, the stronger the influence of

topography (Bayer et al. 1991, Hinse et al. 1988, van Zyl 1993). Because SAR satellites repeat coverage as often as every three days, a considerable amount of fine temporal resolution data may be acquired to monitor ecosystem conditions, which vary on daily to weekly time scales.

Synthetic aperture radar imagery

Most imaging radar sensors operate in a specific band within the microwave wavelength range between approximately 1 cm and 150 cm (Table 1). A digital SAR image consists of a two-dimensional array of picture elements (pixels) with the intensity (called the brightness) of each pixel proportional to the power of the microwave pulse reflected back from the corresponding ground cell. The reflected radar signal is proportional to the backscattering coefficient (σ^0) of a given ground cell, which is related to many system properties as well as the distance

SAR on-line

Satellite SAR images may be viewed on the following Internet home pages:

NASA/JPL Imaging Radar at <http://southport.jpl.nasa.gov/>

Alaska SAR Facility at <http://eosims.asf.alaska.edu:12355/>

National Space Development Agency Earth Observing Center at http://hdsn.eoc.nasda.go.jp/guide/guide/satellite/sendata/sar_e.html

RADARSAT at <http://adro.radar1.sp-agency.ca/adrohomepage.html>

ERS-2 at <http://services.esrin.esa.it/specers2.htm>

by Richard H. Waring, JoBea Way, E. Raymond Hunt Jr., Leslie Morrissey, K. Jon Ranson, John F. Weishampel, Ram Oren, and Steven E. Franklin

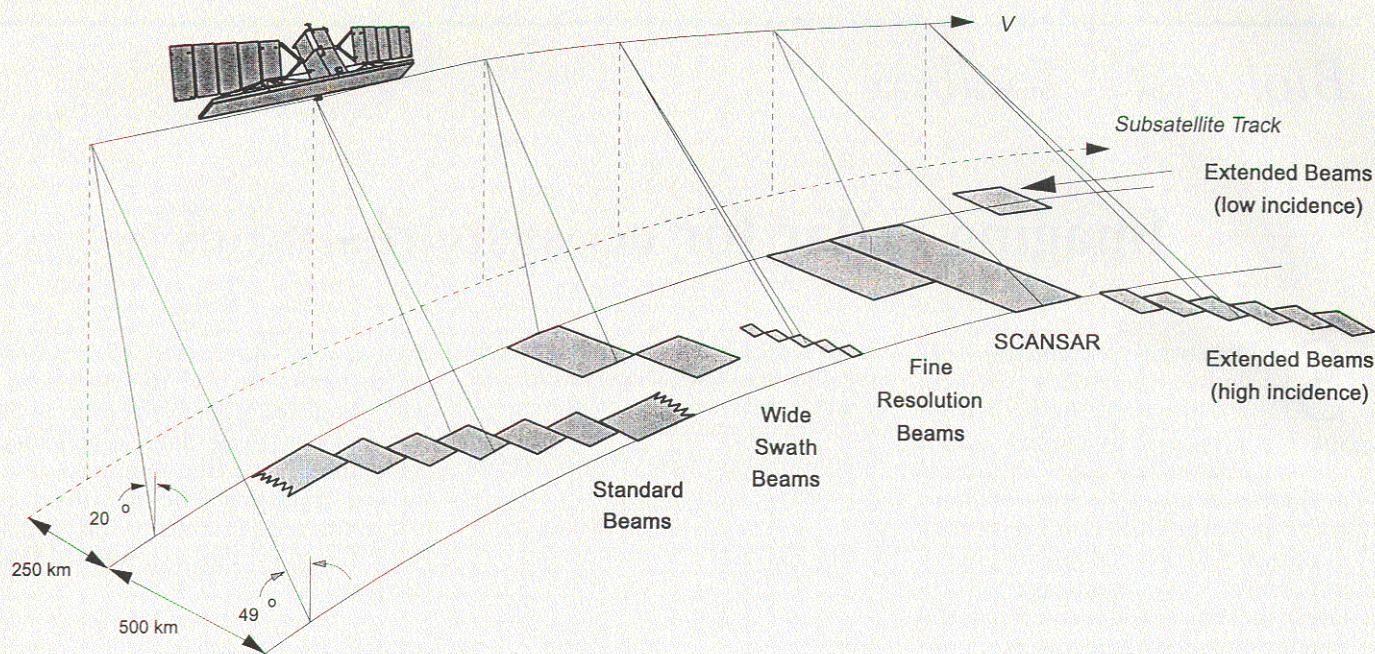


Figure 1. Canadian RADARSAT with synthetic aperture radar acquires backscatter data at various swath widths and incidence angles, which determine the spatial resolution of derived images. After Parashar et al. (1993).

between the radar antenna and the ground cell. Following calibration, the pattern displayed by differences in the brightness among pixels provides a backscatter image. σ^0 is a dimensionless quantity characteristic of the scattering behavior of all the elements contained in a given ground cell. Because σ^0 can vary over several orders of magnitude, it is expressed as a logarithm with units of decibels (dB).

Backscatter coefficients differ depending on the wavelength or frequency, viewing angle, polarization, and characteristics of the surface features and surface topography (Cimino et al. 1986, van Zyl 1993). The atmosphere is essentially transparent to microwaves, even under most cloudy and rainy conditions, but the choice of wavelength is important for assessing structural features of vegetation. Shorter wavelengths (e.g., X- and C-band) carry information related to foliage and small branches. Intermediate L-band wavelengths are sensitive to stems and large branches, whereas the longest wavelengths (P-band) afford the greatest penetration through vegetation and mainly reflect off large stems and the soil surface.

The most advanced radar systems transmit and receive pulses as dif-

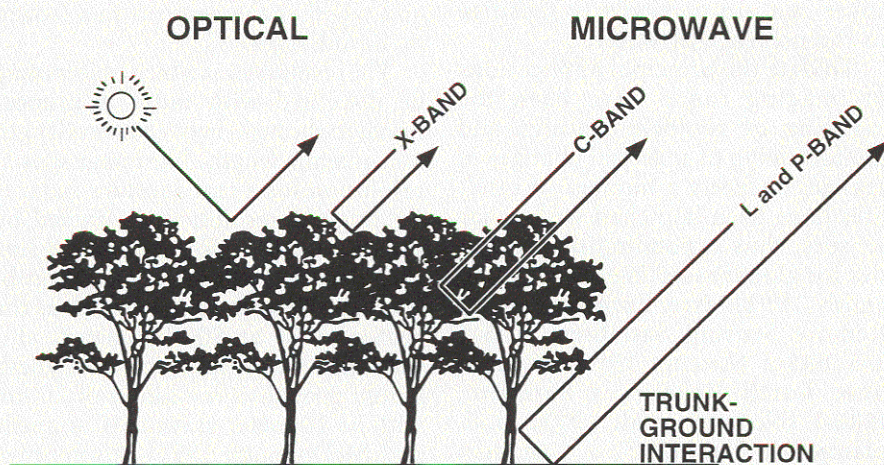


Figure 2. Primary interactions of X-, C-, L-, and P-band microwave with forest canopies. Optical reflectance from the top of the canopy is also shown. After Jet Propulsion Laboratory (1986).

ferent polarizations, which increases the information content in backscatter images. Polarization results because there is an electric field associated with a microwave signal that is perpendicular to the direction of its propagation. If the electric field is transmitted or received parallel to the ground surface, the signal is referred to as horizontally polarized. When the polarized signal is transmitted or received so that the electric field is at a right angle to the surface, the electrical field is

vertically polarized. A signal that reflects off a tree trunk to the ground surface before returning to the radar antenna is likely to show distinctive polarization shifts from signals that return directly off the soil. Surface objects that scatter microwaves, if vertically oriented (e.g., wheat stalks), show high backscatter in vertically polarized imagery and low backscatter in horizontally polarized imagery.

Microwave signals are influenced not only by the shape, density, and

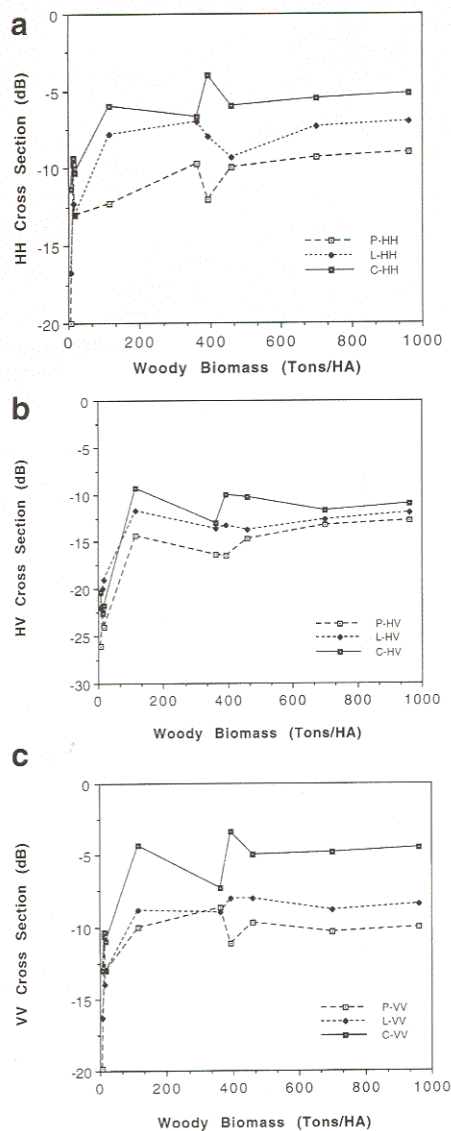


Figure 3. Three radar bands C, L, and P that were generated and received in electrical polarized fields oriented at (a) horizontal (HH), (b) cross (HV), and (c) vertical (VV) directions to the ground indicate that biomass in coniferous forests of the Pacific Northwest could not be assessed accurately above values of 150 Mg/ha. After Moghaddam et al. (1994).

orientation of objects in the scene but also by the dielectric characteristics of surface features. Dielectric properties are a measure of the rotation of polar molecules such as water. Thus, the more liquid water contained in a surface material, the greater the microwave reflection. If the surface substance is frozen, it no longer scatters microwaves because the water molecules no longer rotate and the dielectric constant is reduced accordingly.

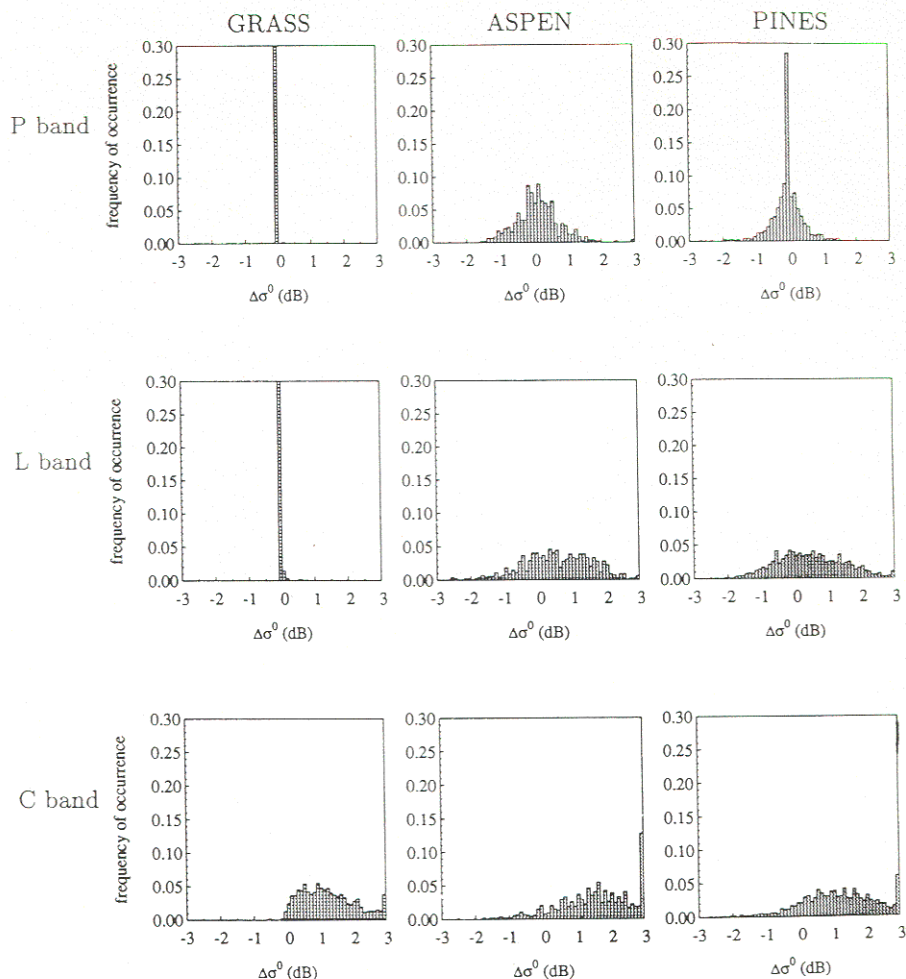


Figure 4. Aircraft-borne radar with C-, L-, and P-bands and HH polarization showed shifts ($\Delta\sigma^0$) in the frequency distribution of backscatter coefficients from wet (8 July 1990) to dry conditions (10 July 1990) for three distinct types of vegetation. Shifts in backscatter coefficients were largest for C-band and least for P-band. After Ulaby and Dobson (1993).

Structural features of vegetation

Ecologists are interested in recognizing structural properties that characterize different vegetation types, in mapping the presence of gaps in canopies, and in assessing the area coverage of leaves or total aboveground biomass. SAR contributes extensively to these objectives.

Estimating standing biomass. Optical sensors are unable to distinguish differences in standing biomass where vegetation is dense (Christensen and Goudriann 1993, Cohen and Spies 1992, Wu and Strahler 1994). Because longer microwave wavelengths penetrate through the

leafy canopy (Figure 2), radar holds more promise for assessing standing woody biomass than do optical sensors. Studies using single wavelength data show that present detection limits are between 100 to 150 Mg/ha (Figure 3; Beaudoin et al. 1993, Dobson et al. 1992b, Moghaddam et al. 1994, Sader 1987). By using a combination of radar bands and polarizations, detection limits may be increased to 250 Mg/ha as demonstrated for a mixture of northern hardwoods and conifers (Ranson and Sun 1994a) and perhaps even higher when trees are frozen or leafless (Ahern et al. 1991). Multiband radars are not yet available on any satellite. Additional knowledge concerning the type and structure of the

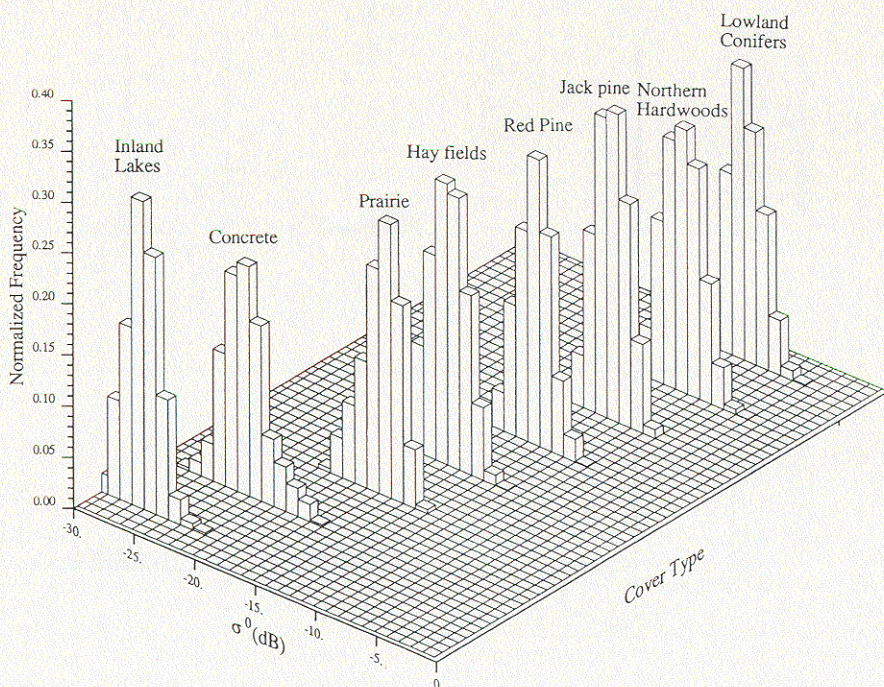


Figure 5. Satellite-borne radar (ERS-1) with C-band and VV polarization distinguished major cover types in Michigan on a single day when leaf surfaces were dry based on backscatter distributions collected from nine scene elements, each 37×37 m. After Dobson et al. (1992a). © 1992 The Institute of Electrical and Electronics Engineers.

local vegetation is required to make predictions of biomass above 150 Mg/ha with the most sophisticated models, which separately account for crown and stem biomass (Dobson et al. in press).

The application of SAR for estimating standing biomass varies by region. In the boreal forests where growth is slow and the vegetation is often sparse, single L- or P-band radar can distinguish a nearly full range of biomass represented in different successional stages of vegetation (Kasischke et al. 1994). On the other hand, in wet tropical forests where regrowth after ten years may reach 400 Mg/ha, biomass detection limits are quickly exceeded as forests reclaim abandoned land (Nepstad et al. 1991). In the giant coniferous forests of the Pacific Northwest, where old-growth forests average 800–1000 Mg/ha and redwoods can reach 2500 Mg/ha (Waring and Franklin 1979), most of the heavily forested areas exceed detection limits, as indicated in Figure 3.

Leaf area index. Leaf area index and foliar biomass are related variables

important in estimating solar energy interception, photosynthesis, evapotranspiration, and mineral cycling in ecosystems (Pierce et al. 1994). Optical sensors on present satellites can follow changes in leaf area index seasonally under cloud-free conditions but are sensitive to atmospheric variations and low sun angles. In regions where the dominant vegetation is coniferous forest, optical sensors can estimate leaf area indices (one-sided or projected) up to values of 6 (Spanner et al. 1994). Where mixed vegetation is present, neither leaf area index nor foliage biomass is easily assessed because of variation in leaf orientation and canopy architecture. However, the fraction of photosynthetically active radiation intercepted by canopies, which is an exponential function of leaf area index, is a linear function of the most common optical reflectance index of green vegetation (Asrar et al. 1992, Goward and Huemmrich 1992, Goward et al. 1994, Law and Waring 1994).

SAR sensors have obvious advantages in being able to distinguish seasonal changes in canopy leaf area,

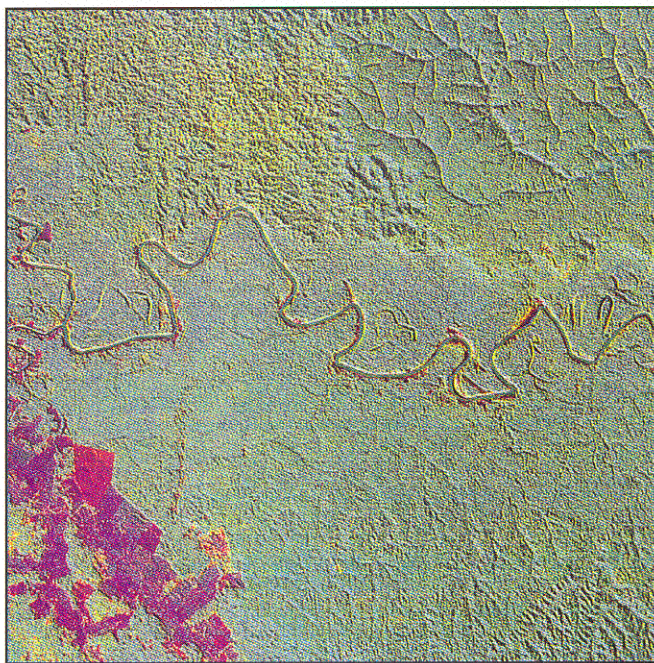
even when persistent cloud cover precludes observations with optical sensors. Variations caused by condensation of fog or dew on leaf surfaces, however, may limit accuracy of leaf area index and foliage biomass estimates with radar (Sader 1987). Differences in leaf display also affect radar signals. Recent studies show that C-band radar from the ERS-1 satellite was unable to quantify leaf area coverage of deciduous species, because the horizontal orientation of leaves severely limits C-band penetration. On the other hand, the more dispersed foliage of needle-leaf coniferous allowed assessment of leaf area index up to values of 4 (Franklin et al. 1994, Ulaby and Dobson 1993).

Distinguishing vegetation types.

Broadly differing life-forms, such as grass meadows, deciduous forests, and coniferous forests, exhibit distinct backscattering properties for selected radar bands. By comparing differences in backscattering coefficients ($\delta\sigma^0$) when foliage is wet to when it is dry, the resulting frequency distribution of the various radar bands can separate major types of vegetation (Figure 4). The shorter C-band wavelength is particularly sensitive to wet canopies, whereas the longer wavelengths (L- and P-bands) are not. Under dry conditions, C-band radar can distinguish major land-cover categories when the frequency distribution of a 3×3 pixel array representing a given type are compared (Figure 5). The smooth surface of lakes produced the lowest backscatter (approximately -26 dB), with concrete surfaces slightly higher (-23 dB). Prairie and hayfields averaged approximately -16 dB, whereas forests separated into two broad groups: upland conifers (between -11 dB and -13 dB) and others (more than -10 dB). Coverage with multi-band radar and combinations of polarization offer the greatest potential for mapping forests types that include deciduous hardwoods and various coniferous species (Rignot et al. 1994b).

A classification accuracy of up to 66% was reported by Ranson and Sun (1994b) in a mapping scheme that included classes of forests of pure hardwoods and conifers, for-

Figure 6. By combining C-band radar with optical data obtained from a LANDSAT image of the western Amazon Basin in Brazil, topographic features provided from radar are complemented by vegetation changes assessed optically. Along the flood-plain of the large river where abandoned meanders are visible, a young closed canopy of rain forest is present. An older, closed rain forest occupies the upper right corner of the image, whereas a more open forest with a bamboo understory dominates the upper left portion. Human disturbance associated with farming and pasturing is indicated in the lower left corner of the scene. After Ahern et al. (1993b).



ests of mixed composition, young regenerating forests, bogs, and open water observed in a single summer scene. Drieman (1994) demonstrated that C-band SAR provided reasonable accuracy in discriminating major forest types and recently cleared forests in eastern Canada and suggested that forest type inventories in that region may be completed with imaging radar data alone. Additional improvements in accuracy can be obtained using multitemporal and seasonal SAR imagery (Ahern et al. 1993a, Ranson and Sun 1994b). Where topography is highly variable, radar imagery can still be valuable for classification if combined with digital elevation data (Peddle and Franklin 1991) or with information derived with optical remote sensing (Figure 6; Evans and Milton 1991, Paris and Kwong 1988).

Distinguishing canopy gaps. Recently developed spatially explicit successional models (Urban et al. 1991, Weishampel et al. 1992) require information concerning the size and shape of canopy gaps, as well as the frequency at which they are formed. Areas devoid of tree cover characteristically exhibit low radar backscatter associated with

relatively smooth surfaces, or in the case of optical sensors, lower values of canopy greenness. Sometimes, however, backscattering may be enhanced if tree cover is sparse but uniformly distributed, because radar beams bounce back and forth between the ground and isolated tree trunks (Ranson and Sun 1993, Richards et al. 1987a).

As gap size decreases, the ability of radar to discern differences becomes more problematic, depending a great deal on the uniformity of the ground surface and uniformity in spacing of trees (Westman and Paris 1987). In some cases, the presence of gaps smaller than the pixel resolution can be mapped; the limits on this procedure are still under study with detailed backscatter models (Sun and Ranson 1995). In cases where radar analyses can be coupled with well-designed ground surveys, classifications of various features can be improved with texture analyses of radar images (Sheen and Johnston 1992, Ustin et al. 1991, Weishampel et al. 1994).

Assessing water limitations

Structural information is essential for initializing, calibrating, and vali-

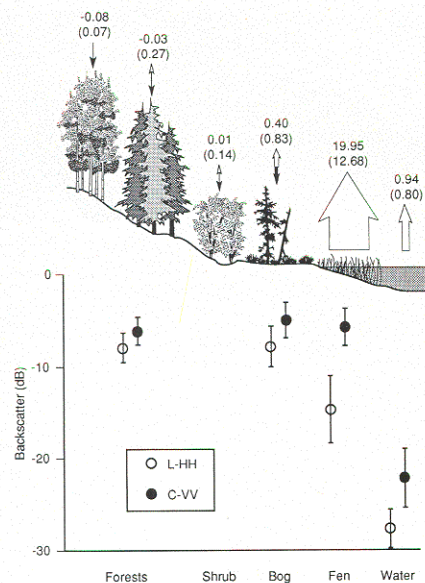


Figure 7. Ground-measured methane exchange rates (mean values and standard deviations shown above vegetation in $\text{mg CH}_4 \times \text{m}^{-2} \times \text{hr}^{-1}$) correlate with backscatter coefficients obtained with airborne C- and L-band microwaves sent and received, respectively, in vertically (VV; ●) and horizontally (HH; ○) polarized electrical fields across a range of taiga vegetation. The data indicate that the major source of methane emissions is fen vegetation, which is dominated by sedge plants. After L. Morrissey, unpublished data.

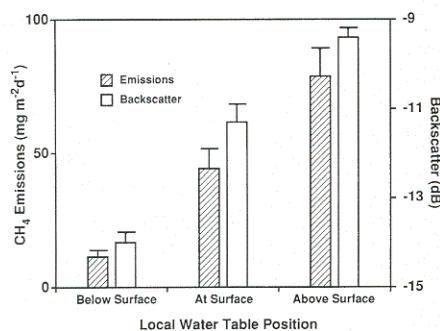


Figure 8. C-band radar backscatter measured from the European Earth Remote Sensing Satellite (ERS-1) correlate well with position of the water table above the surface of sedge-dominated fen vegetation and methane exchange rates in the tundra. Mean values with standard error are shown. After Morrissey et al. (1994).

dating ecosystem and succession models. Estimating the rates at which minerals, water, and energy are cycled through ecosystems and forest communities require some additional information about the environment. Because water is essential

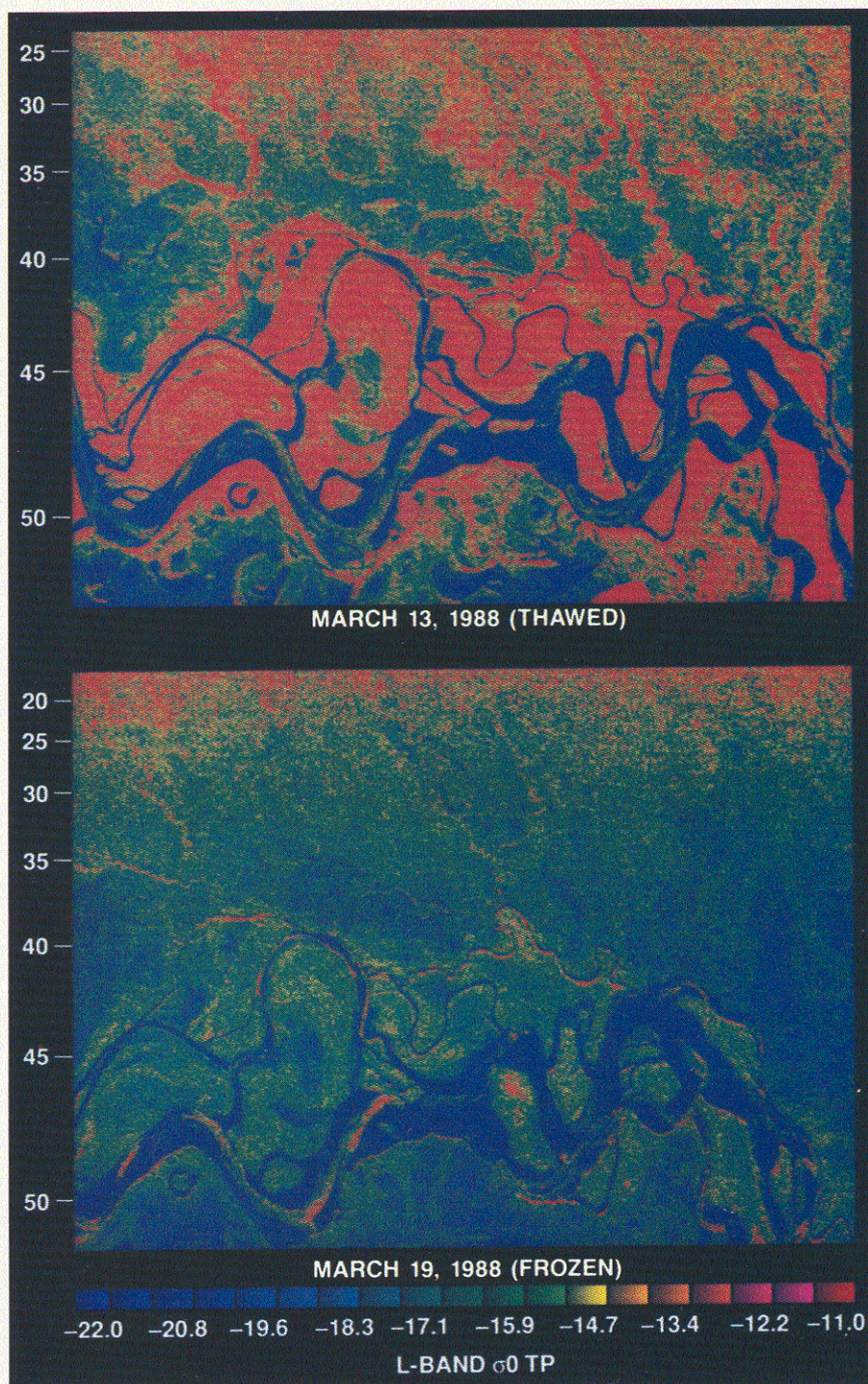


Figure 9. Airborne L-band radar shows the effect of changes in the dielectric constant of water in liquid and frozen states of images acquired five days apart (13 and 19 March 1988) over the Bonanza Creek Experimental Forest, an established Long-Term Ecological Research site, near Fairbanks, Alaska. After Way et al. (1994).

for all of life's processes, and because radar is sensitive to changes in the amount and state of water through the dielectric constant, it is logical to investigate whether radar remote sensing can assess variations in the state of water on sur-

faces and within plants, litter, and soil.

Assessing flooded conditions. In many areas, flooding occurs periodically, and at these times cloud cover usually obscures all observa-

tions with optical or thermal sensors. The smooth surface of standing water reflects all incident microwave radiation away from the sensor, resulting in a much lower backscatter than a dry surface. Under vegetation, a unique corner-reflection backscatter interaction between surface water and tree stems results in an extremely high backscatter and allows inundation to be clearly mapped (Hess et al. 1990, Richards et al. 1987b).

The presence of shallow water is indicative of anaerobic conditions, which under certain conditions favor the production of methane and other trace gases. The transport of gases to the surface is greatly enhanced through hollow-stemmed plants (e.g., reeds, sedges, and rice), making wetlands a major source of trace gases. Because of the vertical orientation of these kinds of plants and the underlying surface water, radar backscatter properties can identify the most active sites for trace gas emission and predict seasonal variation in gas exchange associated with the position of the water table (Figures 7 and 8; Morissey et al. 1994).

Assessing frozen conditions. Ice formation in soil and within the stems of vascular plants clearly limits most hydraulic and physiologic processes. In many regions, freezing conditions set limits on the growing season of crops as well as other vegetation. Dense canopies of vegetation shield against radiation frost but may also extend the period that snow remains present. Differences in the radiative reflective properties of stems and branches and in the osmotic properties of cells can alter the extent of freezing as well. Consequently, it is desirable to have an independent measure of freezing conditions beyond that provided from weather records.

Radar, because of its sensitivity to changes in the dielectric constant of water, has shown potential for mapping freeze-thaw conditions over wide areas (Rignot and Way 1994, Rignot et al. 1994a, Way et al. 1991, 1994). When water is frozen within wood, the dielectric constant changes from approximately 30 to less than 5 (Way et al. 1991). The resulting change in backscatter is

significant (Figure 9). Data collected over boreal forests in Alaska from an aircraft with L-band radar showed a significant drop in backscatter when freezing occurred in boreal vegetation (Way et al. 1994). The ERS-1 satellite equipped with a C-band radar also has shown the ability to distinguish frozen from thawed conditions on a local and regional basis (Rignot and Way 1994, Rignot et al. 1994a).

Assessing moisture stress in vegetation. During daylight hours, transpiration by woody plants may exceed water uptake by a third, even in maritime climates (Waring et al. 1980). The water deficit is met primarily through temporary extraction from water-filled conducting elements in the sapwood of branches and stems. The extraction of water from the conducting elements increases the hydraulic resistance and thereby causes reductions in photosynthesis and transpiration (Waring and Silvester 1994). In dense coniferous forests, the sapwood in stems and branches holds up to a ten-day reserve of water (Waring and Running 1978).

In experiments where water has been sprayed on conifer and hardwood trees during the peak of daily transpiration, rapid changes in water potential, dielectric constants, and water flux through the sapwood have been measured (Figure 10). Lags in the response of water potential to changes in water flux are indicative of likely changes in water storage in the sapwood (McDonald et al. 1992). Dielectric changes of more than 30 units have been measured in the most active outer sapwood near the base of the tree, suggesting changes in the fraction of free-water in conducting elements (McDonald et al. 1990, Way et al. 1991). When radar measurements have been made in conjunction with such studies, the backscattering coefficients change 1–3 dB (McDonald et al. 1990, Ulaby and Dobson 1993). Repeated measurements of backscatter over a season may be required to provide evidence of persistent drought associated with reductions in stem water content.

Assessing soil moisture. The moisture content of soils greatly affects

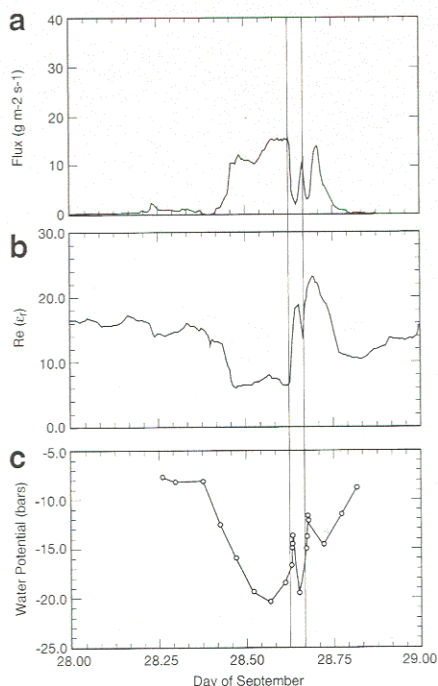


Figure 10. Important changes in the water relations of a *Deodara* cypress tree occurred when the crown was sprayed with water for slightly more than four minutes, noted as the period between two vertical parallel lines. Almost immediately, the flux of water through the stem dropped (a), followed by an increase in the dielectric constant (ϵ_r) of wood (b), and a recovery in twig water potential (c). The large variation in dielectric constant is indicative of changing water content. After McDonald et al. (1992). © 1992 The Institute of Electrical and Electronics Engineers.

water uptake by plant roots and the rates of microbial activities. It is therefore an important variable in all ecosystem models. Radar is limited in its ability to measure soil water content to the upper soil layers. L-band radar only penetrates into bare, damp, smooth soil to a maximal depth of 10 cm. Shorter wavelengths penetrate to only 1–3 cm. In agricultural fields that have smooth soil surfaces and biomass of less than 1 Mg/ha, moisture content of surface layers can be fairly accurately determined (Dobson et al. 1992b, Engman 1991, Jackson and Schmugge 1991, Ulaby and Dobson 1993, Wang et al. 1994). Once vegetation exceeds the biomass limit, however, the ability of radar to sense surface soil water conditions rapidly decreases. The presence of dead vegetation also contributes to at-

tenuating the backscattering signal (Engman 1991). Under a forest canopy, the amount of moisture held in the leaves is so large that it interferes with any direct assessment of soil water status (Jackson and Schmugge 1991). In more open savanna, the predominant source of water during drought periods is well below the surface 10 cm and thus not discernible by radar.

Alternatively, moisture conditions under forests can be inferred using a combination of optical and thermal bands when the analysis is made across of a range of canopy densities during extended drought periods (Goward et al. 1994, Nemani and Running 1989, Nemani et al. 1993). Comparable area-wide analyses have not been made with radar except to document flooding or freezing conditions.

Conclusions

Imaging radar provides a sensitive means of remotely sensing the extent and duration of flooding under a range of types of cover vegetation. Likewise, when water freezes in vegetation and soil, changes in backscatter can readily be detected with radar. Persistent drought that results in reducing water content of leaves and stems of vegetation may also be detected with repeated radar coverage. Radar is limited in its ability to quantify soil moisture at depths below 10 cm or when vegetation exceeds 1 Mg dry matter/ha.

Current space-borne imaging radars can assess structural features, such as leaf area index in conifer forests up to a leaf area index of 4, which is slightly below the sensitivity obtained with optical sensors. Many ecosystem models calculate water vapor and carbon dioxide exchange from vegetation based on the interception of radiation. Both optical and radar sensors provide better and more general estimates of the fraction of radiation intercepted than they do of leaf area index. With a single radar band, biomass detection limits are generally less than 150 Mg/ha. With additional bands, detection limits may be increased slightly but are still well below that desired for global surveys of tropical and temperate for-

ests where standing biomass values usually exceed 400 Mg/ha. The ground resolution of airborne SAR is 1–10 m; the resolution from present imaging radar satellites is 10–30 m. Some gaps within forest canopies can be recognized at sizes well below the pixel resolution in backscatter images. Radar, when combined with optical and thermal remote sensing, provides independent estimates of many important ecological variables and complementary data, which can increase the reliability and value of remote sensing to many ecosystem studies.

Acknowledgments

Diane Wickland, manager for the NASA Terrestrial Ecology Program, commissioned a workshop for the production of this article. Craig Dobson hosted the workshop at the University of Michigan's Biological Station. Ghassem Asrar at NASA Headquarters provided encouragement for this endeavor. To these people and to Kyle McDonald, Janet Franklin, and Diane Evans who reviewed earlier drafts of the manuscript, we are most grateful.

References cited

- Ahern FJ, Skelly WC, McDonald K, Pearce C. 1991. Studies of microwave sensitivity to black spruce biomass with the MIMICS model. Pages 252–258 in Franklin SE, Thompson DM, Ahern FJ, eds. Proceedings of the 14th Canadian Symposium on Remote Sensing. Calgary (Alberta): Canadian Remote Sensing Society.
- Ahern FJ, Leckie DG, Drieman JA. 1993a. Seasonal changes in relative C-band backscatter of northern forest cover types. IEEE Transactions on Geoscience and Remote Sensing 31: 668–680.
- Ahern FJ, Leckie DG, Werle D. 1993b. Applications of RADARSAT SAR data in forested environments. Canadian Journal of Remote Sensing 19: 330–337.
- Asrar G, Myneni RB, Chodhury BJ. 1992. Spatial heterogeneity in vegetation canopies and remote sensing of absorbed photosynthetically active radiation: a model study. Remote Sensing of Environment 41: 85–103.
- Attema E. 1991. The active microwave instrument on-board the ERS-1 satellite. Proceedings of the IEEE 79: 791–799.
- Beaudoin A, Le Toan T, Hsu CC, Kong JA. 1993. Estimation de la Biomasse ligneuse de forêts de pin maritime à l'aide de données radar. Pages 205–270 in Gagnon P, O'Neill N, eds. Proceedings of the 16th Canadian Symposium on Remote Sensing. Sherbrooke (Quebec): Canadian Remote Sensing Society and Metrolitho Inc.
- Christensen S, Goudriann J. 1993. Deriving light interception and biomass from spectral reflectance ratio. Remote Sensing of Environment 43: 87–95.
- Cimino JB, Brandani A, Casey D, Rabassa J, Wall S. 1986. Multiple incidence angle SIR-B experiment over Argentina: mapping of forest units. IEEE Transactions on Geoscience and Remote Sensing 24: 498–509.
- Cohen WB, Spies TA. 1992. Estimating structural attributes of Douglas-fir/western hemlock forest stands from Landsat and SPOT imagery. Remote Sensing of Environment 41: 1–17.
- Curlander JC, McDonough RN. 1991. Synthetic Aperture Radar: systems and signal processing. New York: John Wiley & Sons.
- Danson FM, Curran PJ. 1993. Factors affecting the remotely sensed response of coniferous forest plantations. Remote Sensing of Environment 43: 55–65.
- Dobson MC, Pierce L, Sarabandi K, Ulaby FT, Sharik T. 1992a. Preliminary analysis of ERS-SAR for forest ecosystem studies. IEEE Transactions on Geoscience and Remote Sensing 30: 203–211.
- Dobson MC, Ulaby FT, LeToan T, Beaudoin A, Kasischke ES, Christensen N. 1992b. Dependence of radar backscatter on coniferous forest biomass. IEEE Transactions on Geoscience and Remote Sensing 30: 412–415.
- Dobson MC, et al. In press. Estimation of forest biophysical characteristics in northern Michigan with SIR-C/X-SAR. IEEE Transactions on Geoscience and Remote Sensing.
- Drieman JA. 1994. Forest cover typing and clearcut mapping in Newfoundland with C-band SAR. Canadian Journal of Remote Sensing 20: 11–16.
- Engman ET. 1991. Application of microwave remote sensing of soil moisture for water resources and agriculture. Remote Sensing of Environment 35: 213–226.
- Evans DL, Milton MO. 1991. Separation of vegetation and rock signatures in Thematic Mapper and polarimetric SAR images. Remote Sensing of Environment 37: 63–75.
- Franklin SE, Lavigne MB, Wilson BA, Hunt ER Jr. 1994. Empirical relations between balsam fir (*Abies balsamea*) fir stand conditions and ERS-1 SAR data in western Newfoundland. Canadian Journal of Remote Sensing 20: 124–130.
- Goward SN, Huemmrich KF. 1992. Vegetation canopy PAR absorptance and the normalized difference vegetation index: an assessment using the SAIL model. Remote Sensing of Environment 39: 119–140.
- Goward SN, Waring RH, Dye DG, Yang J. 1994. Ecological remote sensing at OTTER: satellite macroscale observations. Ecological Applications 4: 322–343.
- Hess LL, Melack JM, Simonett DS. 1990. Radar detection of flooding beneath the forest canopy: a review. International Journal of Remote Sensing 5: 1313–1325.
- Hinse M, Gwyn Q, Bonn F. 1988. Radiometric correction of C-band SAR imagery for topographic effects in regions of moderate relief. IEEE Transactions on Geoscience and Remote Sensing 26: 122–132.
- Jackson TJ, Schmugge TJ. 1991. Vegetation effects on microwave emission of soils. Remote Sensing of Environment 36: 203–212.
- Jet Propulsion Laboratory. 1986. Shuttle Imaging Radar—C science plan. Jet Propulsion Laboratory Publication 86–29.
- Kasischke ES, Bourgeau-Chavey LL, Christensen NL Jr., Haney E. 1994. Observations on the sensitivity of ERS-1 SAR image intensity to changes in above-ground biomass. International Journal of Remote Sensing 15: 3–16.
- Law BE, Waring RH. 1994. Combining remote sensing and climatic data to estimate net primary production across Oregon. Ecological Applications 4: 717–728.
- McDonald KC, Dobson MC, Ulaby FT. 1990. Using MIMICS to model L-band multi-angle and multi-temporal backscatter from a walnut orchard. IEEE Transactions on Geoscience and Remote Sensing 28: 477–491.
- McDonald KC, Zimmermann R, Way JB, Oren R. 1992. An investigation of the relationship between tree water potential and dielectric constant. Pages 533–525 in Proceedings of the 1992 International Geoscience and Remote Sensing Symposium. Clear Lake (TX): The Institute of Electrical and Electronics Engineers.
- Moghaddam M, Durden S, Zebker H. 1994. Radar measurement of forested areas during OTTER. Remote Sensing of Environment 47: 154–166.
- Morrissey LA, Livingston GP, Durden SL. 1994. Use of SAR in regional methane exchange studies. International Journal of Remote Sensing 15: 1337–1342.
- Nemani RR, Running SW. 1989. Estimation of surface resistance to evapotranspiration from NDVI and thermal-IR AVHRR data. Journal of Applied Meteorology 28: 276–294.
- Nemani RR, Running SW, Pierce LL, Goward SN. 1993. Developing satellite derived estimates of surface moisture status. Journal of Applied Meteorology 32: 548–557.
- Nemoto Y, Nishino H, Ono M, Mizutamari H, Nishikawa K, Tanaka K. 1991. Japanese Earth Resources Satellite-1 Synthetic Aperture Radar. Proceedings of the IEEE 79: 800–809.
- Nepstad DC, Uhl C, Serrao EAS. 1991. Recuperation of a degraded Amazonian landscape: forest recovery and agricultural restoration. Ambio 20: 248–255.
- Parashar S, Langham E, McNally J, Ahmed S. 1993. Radarsat mission requirements and concept. Canadian Journal of Remote Sensing 19: 280–288.
- Paris JF, Kwong H. 1988. Characterization of vegetation with combined Thematic Mapper (TM) and Shuttle Imaging Radar (SIR-B) data. Photogrammetric Engineering and Remote Sensing 54: 1187–1193.
- Peddle DR, Franklin SE. 1991. Image texture processing and data integration for improved surface discrimination. Photogrammetric Engineering and Remote Sensing 57: 413–420.
- Pierce LL, Running SW, Walker J. 1994. Regional scale relationships of leaf area

- index to specific leaf area and leaf nitrogen content. *Ecological Applications* 4: 313–321.
- Ranson KJ, Sun G. 1993. Retrieval of forest spatial patterns from SAR images. Pages 1212–1215 in *International Geoscience and Remote Sensing Symposium*, Tokyo, Japan, Aug 17–20.
- _____. 1994a. Mapping biomass of a northern forest using multifrequency SAR data. *IEEE Transactions on Geoscience and Remote Sensing* 32: 388–396.
- _____. 1994b. Northern forest classification using temporal multifrequency and multipolarimetric SAR images. *Remote Sensing of Environment* 47: 142–153.
- Richards JA, Sun G-Q, Simonett DS. 1987a. L-band backscatter modeling of a forest stand. *IEEE Transactions on Geoscience and Remote Sensing* 25: 487–498.
- Richards JA, Woodgate PW, Skidmore AK. 1987b. An explanation of enhanced radar backscattering from flooded forests. *International Journal of Remote Sensing* 8: 1093–1100.
- Rignot E, Way JB. 1994. Monitoring freeze-thaw cycles along north-south Alaskan transects using ERS-1 SAR. *Remote Sensing of Environment* 49: 131–137.
- Rignot E, Way JB, McDonald K, Viereck L, Williams C, Adams P, Payne C, Wood W, Shi J. 1994a. Monitoring environmental conditions in taiga forests using ERS-1 SAR data: results from the Commissioning Phase. *Remote Sensing of Environment* 49: 145–154.
- Rignot E, Williams C, Way JB, Viereck L. 1994b. Mapping of forest types in Alaskan boreal forests using SAR imagery. *IEEE Transactions on Geoscience and Remote Sensing* 32: 1117–1124.
- Sader SA. 1987. Forest biomass, canopy structure, and species composition relationships with multipolarization L band synthetic aperture radar data. *Photogrammetric Engineering and Remote Sensing* 53: 193–202.
- Sheen DR, Johnston L. 1992. Statistical and spatial properties of forest clutter measured with polarimetric synthetic aperture radar. *IEEE Transactions on Geoscience and Remote Sensing* 30: 578–588.
- Spanner M, Johnson L, Miller J, McCreight R, Runyon J, Gong P, Pu R. 1994. Remote sensing of seasonal leaf area index across the Oregon transect. *Ecological Applications* 4: 258–271.
- Sun G, Ranson KJ. 1995. A three-dimensional radar backscatter model for forest canopies. *IEEE Transactions on Geoscience and Remote Sensing* 33: 372–382.
- Ulaby FT, Dobson MC. 1993. Radar response of vegetation: an overview. Pages 151–183 in *Proceedings of the Third Spaceborn Imaging radar symposium*. Jet Propulsion Laboratory Publication 93–16.
- Urban DL, Bonan GB, Smith TM, Shugart HH. 1991. Spatial applications of gap models. *Forest Ecology and Management* 42: 95–110.
- Ustin SL, Wessman CA, Curtiss B, Kasischke E, Way J, Vanderbilt VC. 1991. Opportunities for using the EOS imaging spectrometers and synthetic aperture radar in ecological models. *Ecology* 72: 1934–1945.
- van Zyl JJ. 1993. The effects of topography on radar scattering from vegetated areas. *IEEE Transactions on Geoscience and Remote Sensing* 31: 153–160.
- Wang Y, Kasischke ES, Melack JM, Davis FW, Christensen NL Jr. 1994. The effects of changes in loblolly pine biomass and soil moisture on ERS-1 SAR backscatter. *Remote Sensing of Environment* 49: 25–31.
- Waring RH, Franklin JF. 1979. Evergreen coniferous forests of the Pacific Northwest. *Science* 204: 1380–1386.
- Waring RH, Running SW. 1978. Sapwood water storage: its contribution to transpiration and effect upon water conductance through the stems of old-growth Douglas-fir. *Plant, Cell and Environment* 1: 131–140.
- Waring RH, Silvester WB. 1994. Variation in foliar $\delta^{13}\text{C}$ values with the crowns of *Pinus radiata* trees. *Tree Physiology* 14: 1203–1213.
- Waring RH, Whitehead D, Jarvis PG. 1980. Comparison of an isotopic method and the Penman-Monteith equation for estimating transpiration from Scots pine. *Canadian Journal of Forest Research* 10: 555–558.
- Way JB, Smith EA. 1991. The evolution of synthetic aperture radar systems and their progression to the EOS SAR. *IEEE Transactions on Geoscience and Remote Sensing* 29: 922–985.
- Way JB, Paris J, Dobson MC, McDonald K, Ulaby FT, Weber JA, Ustin SL, Vanderbilt VC, Kasischke ES. 1991. Diurnal change in trees as observed by optical microwave sensors: the EOS synergism study. *IEEE Transactions on Geoscience and Remote Sensing* 29: 807–821.
- Way JB, Rignot JM, McDonald KC, Oren R, Kwok R, Bonan G, Dobson MC, Viereck LA, Roth JA. 1994. Evaluating the type and state of Alaskan taiga forests with imaging radar data for use in ecosystem models. *IEEE Transactions on Geoscience and Remote Sensing* 32: 353–370.
- Weishampel JF, Urban DL, Shugart HH, Smith JB Jr. 1992. Semivariograms from a forest transect gap model compared with remotely sensed data. *Journal of Vegetation Science* 3: 521–526.
- Weishampel JF, Sun D, Ranson KJ, LeJeune KD, Shugart HH. 1994. Forest textural properties from simulated microwave backscatter: the influence of spatial resolution. *Remote Sensing of Environment* 47: 120–131.
- Westman WE, Paris JF. 1987. Detecting forest structure and biomass with C-band multipolarization radar: physical model and field tests. *Remote Sensing of Environment* 22: 249–269.
- Wu Y, Strahler AH. 1994. Remote estimation of crown size, stand density and biomass on the Oregon transect. *Ecological Applications* 4: 299–312.

Richard H. Waring is Distinguished Professor of Forest Science in the College of Forestry, Oregon State University, Corvallis, OR 97331-7501. JoBea Way is a research scientist at the Jet Propulsion Laboratory, California Institute of Technology, Pasadena, CA 91109. E. Raymond Hunt Jr. is an assistant professor at the University of Montana, School of Forestry, Missoula, MT 59812. Current address: Department of Botany, University of Wyoming, P.O. Box 3165, Laramie, WY 82071-3165. Leslie Morrissey is a research scientist at the NASA Ames Research Center, Moffett Field, CA 94035. K. Jon Ranson is a research scientist at the Goddard Space Flight Center, Greenbelt, MD 20771. John F. Weishampel is an assistant professor in the Department of Biology, University of Central Florida, Orlando, FL 32816-2368. Ram Oren is an associate professor in the School of the Environment, Duke University, Durham, NC 27706. Steven E. Franklin is chairman of the Department of Geography, The University of Calgary, Calgary, Canada AB T2N 1N4.